Polym. Bull. (2011) 66:1111–1123
DOI 10.1007/s00289-010-0401-z

ORIGINAL PAPER

Dimeric liquid crystalline thermosets from azo-containing diglycidyl ether cured by anhydride

De-Wen Zhou · Li-Yan Liang · Man-Geng Lu

Received: 23 August 2010 / Revised: 21 October 2010 / Accepted: 1 November 2010 /

Abstract A series of dimeric liquid crystalline (LC) epoxy monomers containing azobenzene group with central spacers of different lengths were synthesized and structurally characterized by ^{1}H NMR, ^{13}C NMR, and elemental analysis. The mesogenic behavior of these monomers was measured by differential scanning calorimetry (DSC), polarized optical microscopy (POM), and X-ray diffraction (XRD). Like other dimeric LC epoxy monomers, the melting points, clear points, and mesophase of these compounds are influenced by the carbon numbers of central spacers. Anhydride was employed to cure the monomers and LCTs with nematic phase were obtained. Thermal properties, dynamic mechanical properties and UV–Vis spectra of the LCTs were studied. The decomposition of the LCTs occurred near 220 °C and followed three stages. The LCTs also had the natural absorbance bonds of azo compounds.

Keywords Liquid crystalline polymers · Phase behavior · Azo · Thermal properties

---

D.-W. Zhou · L.-Y. Liang · M.-G. Lu
Guangzhou Institute of Chemistry, Chinese Academy of Sciences, Guangzhou 510650, China

D.-W. Zhou · L.-Y. Liang · M.-G. Lu
Key Laboratory of Molecular Engineering of Polymer (Fudan University),
Ministry of Education, Shanghai 200433, China

D.-W. Zhou
Graduate School of Chinese Academy of Sciences, Beijing 10049, China

M.-G. Lu (✉)
No. 368, Xingke Road, Tianhe District, Guangzhou, Guangdong 10049, China
e-mail: mglu@gic.ac.cn

Introduction

Recently, polymers containing azo group have been extensively investigated for scientific interests and potential applications in various photonic devices [1–3]. Azobenzene group is both a mesogenic and chromophoric group. When a liquid crystalline polymer (LCP) containing azobenzene is irradiated by linearly polarized light, the azo groups tend to align perpendicularly to the polarization direction [4]. Moreover, the oriented azobenzene groups will drive the other mesogenic groups around to align to the same direction [5, 6]. It was demonstrated that azo groups undergo photochemical *trans–cis–trans* isomerization and thermal *cis–trans* isomerization. The *trans*-azobenzene units are much easier to form a mesophase than *cis*-units [1]. In azobenzene-containing LCPs, the light-induced *trans–cis* isomerization of azo units induces the collapse of the alignment order [7]. Most of the researches on the azobenzene-containing polymers are about the side-chain LCPs [4]. In the side-chain LCPs, the general main chains are polysiloxanes and polymethacrylates, where the azobenzene groups are usually attached with different length of spacers. The *trans–cis* photoisomerization of azobenzene is independent of the length of spacers [8–10]. The main drawback of side-chain LCPs is the relaxation of the orientation of mesogenic groups. In liquid crystalline thermosets (LCTs), the alignment of the azobenzene groups can be permanently frozen and the information can be stored in the LCTs at high temperatures [11].

LCTs are prepared from the curing of the reactive groups containing mesogens. A LCT is defined as small molecules with mesogens attached to crosslinkings to show LC behavior. Orientation arrangement of the LC phase under such circumstances is frozen since the local mesogenic units are rigidly held in strong covalent structure [12]. Combining advantages of thermosetting materials and liquid crystals, LCTs have many outstanding performances in heat resistance, mechanical properties, optical properties, and dielectric properties. Potential applications of LCTs include high performance composites, non-linear optics, electronics, etc. A large number of studies have been reported on LCTs, and it was found that various mesogens and crosslinking end groups are appropriate for LCT [13].

Dimeric LC epoxy resins are prone to forming smectic-like structures, because the crosslinking sites at the end of mesogens assist in fixing the molecular spacing during curing [14–16]. Several curing agents, such as diamines [15], catalytic curing agents [17], and diisocyanates [18], and so on, were chosen to cure the dimeric epoxy monomers in order to obtain smectic LCTs. Most of these studies are on the azomethine LC epoxy resins, but only a few reports are on the azo-containing resins which may exhibit some unique optic performances.

This study aims to synthesize a series of dimeric LC epoxy resins containing azobenzene and give the relationships between the molecular structure and phase behavior. Anhydride was employed to cure the monomers and the thermal properties, dynamic mechanical properties, and UV–Vis spectra of the LCTs were studied.

Experimental

Materials

4-Aminobezene acid, phenol, α,ω-dibromoalkanes, 18-crown-6, benzyltrimethylammonium chloride (BTMA), sodium nitrate, epichlorohydrin (EC) were obtained from Shanghai Chemical Reagent, Ltd. The curing agent tetrahydrophthalic anhydride (THPA) was purchased from Alfa Aesar and used as received. All solvents were purified by standard procedures.

Measurement

^{1}H NMR and ^{13}C NMR spectra were obtained with a Bruker DRX-400 spectrometer using $CDCl_3$ or dimethyl sulfoxide-d_6 as the solvent and tetramethylsilane as the internal standard. Elemental analysis was carried out with a PE 2400 analyzer. UV–Vis absorption measurements were made using a Shimadzu 2550 UV–Vis spectrophotometer.

Calorimetric measurements were conducted on a Perkin Elmer DSC 7 thermal analyzer with N_2 as a purge gas. Monomers were studied by a heating–cooling–heating model between 50 and 200 °C at a temperature change rate of 10 °C/min. Glass transition temperature was measured from 50 to 150 °C at a heating rate of 10 °C/min. The thermal decomposition of the monomers and cured LCTs was carried out by thermo-gravimetry in flowing nitrogen (30 mL/min) with the heating rate of 10 °C/min from 50 to 650 °C. Samples of 6–8 mg were used.

X-ray diffraction (XRD) measurements were studied with a Rigaku Diffractometer (D/MAX-1200), using monochromatic CuKα radiation (40 kV, 30 mA) and secondary graphite monochromator, with the X-ray scattering intensities detected by a scintillation counter incorporating a pulse-height analyzer. The textures of the LC phases were examined by a polarized light optical microscopy (Caikon Optic Equipment, Shanghai China) equipped with a (CK-300) hot-stage.

Dynamic mechanical analysis (DMA) measurements were performed on a TA/DMA 2980 apparatus by tensile mode. Measures were run from −50 to 200 °C at the heating rate of 5 °C/min at 1 Hz frequency. Nitrogen was the carrier gas, with the flow rate of 30 ml/min.

Synthesis of epoxy monomers E*n*E

The synthetic scheme for E*n*E is shown in Scheme 1. The epoxy monomer could be obtained from several common primary materials, including α,ω-dibromoalkane, BTMA, and EC.

Synthesis of diamines (P1–*n*)

Diamines were synthesized from the reaction of the corresponding α,ω-dibromoalkanes and 4-aminobezene acid in the presence of 18-crown-6 by following a literature procedure [15].

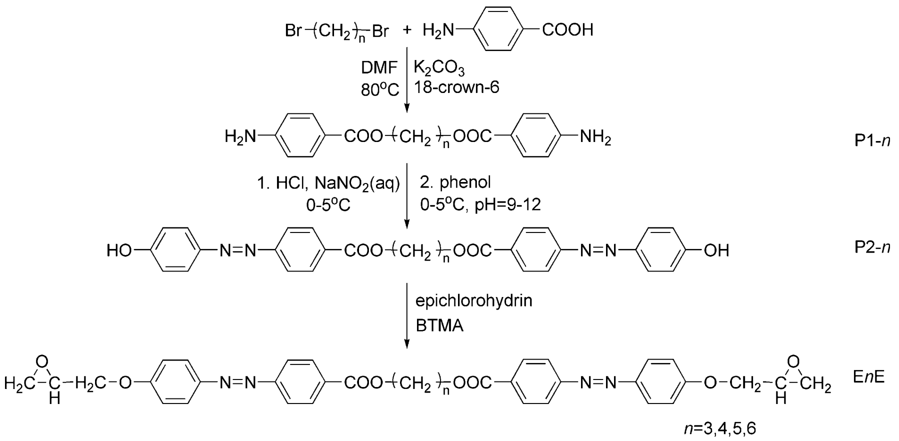

Scheme 1 Synthesis of azo-containing liquid crystalline epoxy monomers

Synthesis of α,ω-bis(4-hydroxylazobenzene-4′-carbonyloxy) alkanes (P2–*n*)

Compound P2–*n* was synthesized according to the classic scheme of diazotization–coupling reaction, as illustrated in Scheme 1. The corresponding α,ω-bis (4-aminobenzoyloxy) alkane (0.025 mol) was suspended in a solution of 10 mL HCl (37 wt%, 0.112 mol) and 150 mL deionized water in a two-necked flask fitted with a magnetic stirrer and cooled to 0–5 °C in an ice-water bath. Under stirring, a solution of 3.6 g sodium nitride (0.052 mol) in 10 mL water was dropped into the flask slowly. After the mixture became clear, stirring continued for 30 min to complete the diazotization of amino group, and then a solution of diazonium salt (solution A) was obtained. A small amount of urea was added to remove the excess nitrous acid. A solution (solution B) containing 4.7 g phenol (0.05 mol) in 250 mL water was prepared and cooled to 0–5 °C in an ice-water bath. Solution A was added dropwise to solution B under stirring, 0.1 M Na_2CO_3 solution was used to control pH = 9–12 and then red-orange precipitation formed from the solution. The precipitation was filtrated and washed twice with water and then twice with methanol. The solid was dried under vacuum. Yield: over 95%. For P2–5, mp: 191–193 °C, yield: 98%, ^{1}H NMR (DMSO-d_6, δ, ppm): 9.30 (s, 2H), 8.16 (d, 4H), 7.88 (m, 8H), 7.02 (d, 4H), 4.39 (t, 4H), 1.92 (t, 4H), 1.71 (t, 2H). ^{13}C NMR (DMSO-d_6, δ, ppm): 165.2, 161.8, 154.7, 145.3, 130.7, 130.3, 125.3, 122.2, 116.0, 64.6, 27.7, 21.9.

Synthesis of diglycidylic compounds (E*n*E)

A mixture of epichloroydrin (5 mol) and the corresponding P2–*n* (0.1 mol) was heated to 110 °C, and solid BTMA (0.01 mol) was added in. The mixture was refluxed and finished in about 1 h. The red homogeneous solution was cooled to room temperature, and then red-orange precipitate was obtained. The solid was filtered off, washed with ether, and dried in vacuum. All of the diglycidylic monomers were recrystallized from toluene twice. Yield: over 80%. For E5E, ^{1}H NMR ($CDCl_3$, δ, ppm): 8.14 (d, 4H), 7.90 (d, 4H), 7.88 (d, 4H), 7.00 (d, 4H), 4.38 (t, 4H), 4.30 (dd, 2H), 4.00 (dd, 2H), 3.39 (m, 2H), 2.92 (t, 2H), 2.78 (dd, 2H), 1.88 (t, 4H), 1.65 (t, 2H). ^{13}C NMR($CDCl_3$, δ, ppm): 166.0, 161.3, 155.1, 147.1, 131.4, 130.4, 125.1, 122.3, 114.8, 68.9, 64.8, 49.9, 44.5, 28.2, 22.5. Elem. Anal. Calcd. for $C_{37}H_{36}N_4O_8$ (664.71). Calcd. C 66.86%, H 5.46%, N 8.43%. Found C 66.73%, H 5.52%, N 8.41%.

Curing of the epoxy resins

The monomers were mixed with stoichiometric THPA by dissolution of the two compounds in anhydrous CH_2Cl_2, and then the solvent was evaporated at room temperature in vacuum. The initial cure of the melted mixture was carried out at the temperature in Table 1 and the post cure was carried at a higher temperature (190 °C) for 1 h.

Molecular geometry calculation

The software Gaussian 03W was employed to estimate the molecular geometry of the monomers. The molecular energy was relaxed by molecular mechanics minimization using *semi*-empirical method provided by Gaussian 03 W. After the complete relaxation of the molecule, the distances between atoms were measured.

Results and discussion

Synthesis and characterization of monomers

Dimeric monomers were synthesized through the well-known reactions given in Scheme 1. The first synthetic step followed the reported procedures with high yield (over 95%) [15]. The second synthetic step involves the diazotization of amino group and the coupling reaction of the diazonium salt with phenol, which are similar to the common synthesis procedure of the azobenzene. The diazotization of amino group was under pH = 2–5 and T = 0–5 °C. After diazotization, small amount of urea was added to remove the residual nitrous acid. The diazonium salt reacted with phenol under pH = 9–11 and T = 0–5 °C. The precipitation of diphenol containing azobenzene was filtrated and washed with water and then with methanol. The coupling reaction leading to azobenzene proceeded almost quantitatively. It was difficult to further purify the diphenols because of their small solubility in general solvents, but the products were pure enough to synthesize the epoxy monomers.

Table 1 The curing conditions of E*n*E–THPA mixtures

Sample	E3E	E4E	E5E	E6E
Curing temperature (°C)	155	180	125	170
Curing time (h)	24	12	36	15

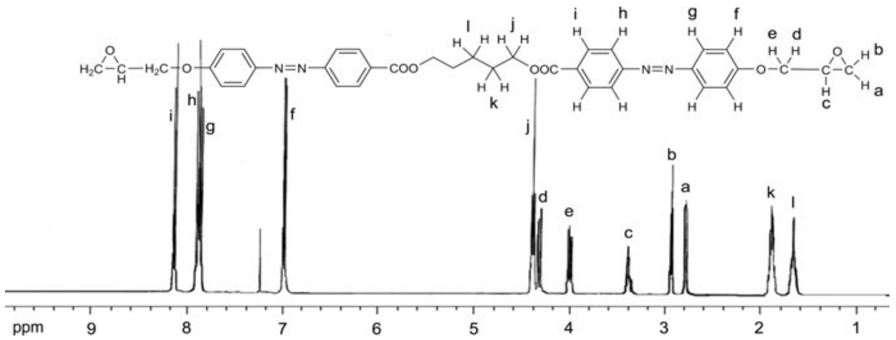

Fig. 1 ^{1}H NMR spectrum of E5E obtained in $CDCl_3$

The monomers E*n*E were obtained by reacting the corresponding diphenols with an excess of epichlorohydrin in the presence of a quaternary ammonium salt, which was similar to the synthesis of azomethine epoxy monomers [15]. Figure 1 shows the ^{1}H NMR spectrum of the epoxy monomer, including the peak assignments corresponding to the structure for the E5E. In the spectrum, the ratio of the peak areas between epoxy protons and four methylene protons attached to moiety appears to be 3:2, which indicates that 2 mol glycidyl ethers obtained consists 1 mol dimeric unit.

Mesophases, structural parameters calculated by Gaussian 03W and XRD data for these monomers are listed in Table 2. The mesophase behavior of these dimeric LC glycidylic monomers was studied by DSC, POM, and XRD. Dimeric LC compounds are prone to form a smectic mesophase. The dimeric LC glycidylic monomers containing azobenzene also exhibit smectic structures. As reported, the ratios *d*/*l* were near 0.5 [15], which means that the mesogens favor an intercalated arrangement to form the smectic-like structures.

The textures of the monomers obtained by POM are shown in Fig. 2. Monomer E3E shows a monotropic smectic C mesophase which can only be observed on

Table 2 Mesophases, structural parameters calculated by Gaussian 03 and X-ray diffraction data for monomers synthesized

E*n*E	Transition temperatures (°C)	Mesophase range S/N (°C)	Terminal chain length (Å)	Half spacer length (Å)	Molecule length *l*[b] (Å)	Layer spacing *d*[c] (Å)	*d*/*l*
E3E	K 164 S_C 183 I[a]	19	4.53	3.60	33.04	14.29	0.43
E4E	K 182 S_A 231 I	49	4.53	4.23	39.30	17.54	0.45
E5E	K 112 S_C 147 N 165 I	35/18	4.53	4.56	34.19	16.82	0.49
E6E	K 161 S_A 193 I	32	4.53	5.47	41.48	20.28	0.49

[a] Monotropic mesophase determinated on cooling from isotropic state

[b] Calculated by Gaussian 03W

[c] XRD

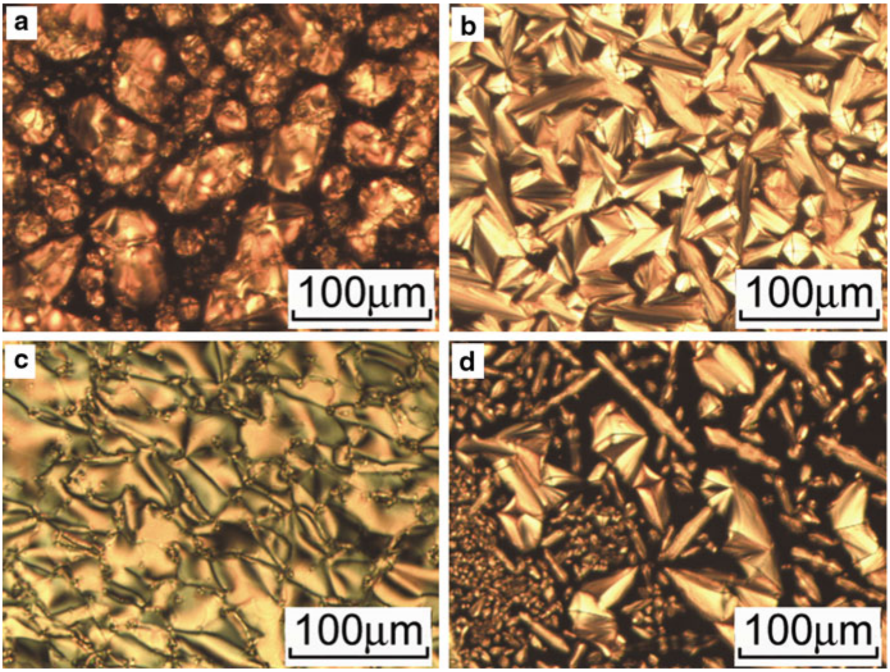

Fig. 2 POM textures of dimeric monomers: **a** E3E at 178 °C on cooling, **b** E4E at 220 °C, **c** E5E at 155 °C, **d** E6E at 179 °C

cooling from isotropic liquid state. E5E shows a smectic C phase between 112–147 °C and a nematic phase between 147–165 °C. For E4E and E6E, only a smectic A mesophase was observed, suggested by the focal conic fan textures (Fig. 1b, d). There are three endothermic peaks on the DSC plot of E5E corresponding to melting transition, smectic C-nematic transition and isotropization (Fig. 3). Schlieren texture of a nematic phase was only observed in E5E.

Curing reaction and phase behaviors

Many hardeners have been applied to cure the dimeric LC epoxy resins, such as diamines, diisocyanates, tertiary amine, and dicarboxylic acids. Anhydrides are usually used as hardeners of epoxy resins for high dielectric properties. In the epoxy-anhydride curing system, initiation reactions are needed and the carboxyl anion reduces the nucleophilic ability, so the reactivity is lower than that of the epoxy-amine systems. The lower reactivity of the anhydride allows longer time for the rearrangement of the mesogens during curing to form LCTs with fewer flaws.

As shown in Fig. 4, there were two endothermic peaks and one exothermic peak during the heating process, which belonged to the melting of the hardener, monomers and curing reaction respectively. The curing reaction E*n*E/THPA mixture without any extra accelerant occurred after the melting of the monomers at about 120 °C (for E5E), which may be catalyzed by the azo group in the monomers.

Fig. 3 DSC curve of monomer E5E at 10 °C/min in N_2

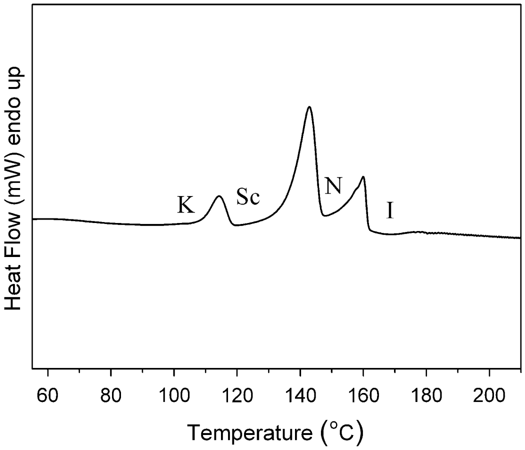

Fig. 4 DSC curves of E*n*E–THPA mixtures at a heating rate of 10 °C/min

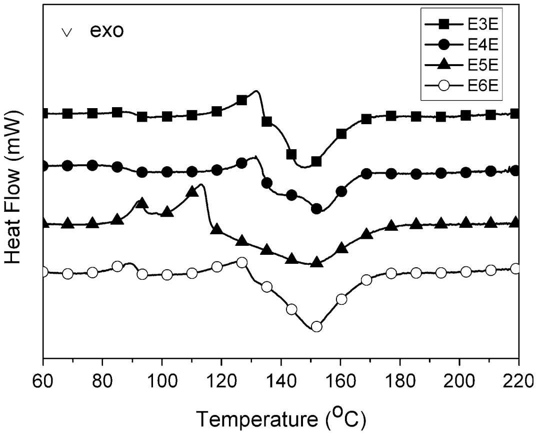

Therefore, LCTs can be obtained by curing E*n*E with an anhydride in the mesophase and without any accelerant. The melting temperature of THPA was matched with the melting points of E*n*E.

The initial phase of all the curing mixtures was nematic with the disappearance of the smetic-like structures of monomers. The nematic phase was frozen in all the LCTs finally. The POM textures and XRD patterns of LCT from E6E–THPA were shown Fig. 5. The smectic textures of E6E disappeared and the nematic phase was confirmed by the POM textures and XRD data. As shown in Fig. 5, the birefringence of LCT can be observed through POM, and the XRD exhibited only one bread-like peak near $2\theta = 19°$, both of which acted as the evidence of nematic phase. The birefringence of the LCT was still kept at a higher temperature (200 °C). The amount of THPA for curing epoxy completely is larger than that of diamines, and too many distortions prevent the molecules from more ordered smectic-like arrangements.

Fig. 5 Wide-angel X-ray diffraction and micrograph of E6E/THPA LCT

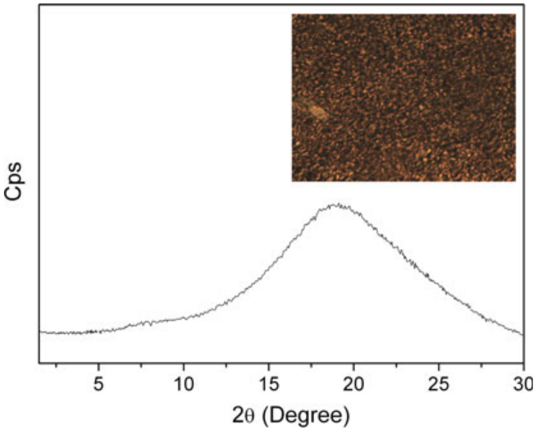

UV–vis absorbance spectrum

Figure 6 makes a comparison of the UV–Vis spectra of the E5E monomer in chloroform and the LCT of E5E–THPA. The peak at ~456 nm is due to the n–π^* transition and the maxima of the absorbance in the range 350–370 nm corresponds to a strong π–π^* electronic transition of the trans-isomer. The E5E showed a typical spectrum of an azo-containing compound. After cured, the absorbent bands of the azo groups were still kept. If the curing reaction was carried under irradiation of polarized light, the azo groups tend to align perpendicularly to the polarization direction and these ordered structures can be permanently frozen in the LCT.

After cured by THPA, the band of the absorbance became wide and had a red shift in comparison with the spectra of the monomer in $CHCl_3$. In the LCTs, the mesogens were surrounded by other mesogens. In our research, an azobenzene mesogen with a carbonyl group and an ether group at each end of the mesogen, respectively, showed a resonance form like the imine group in the reference [15]. The polarity of the surroundings increased due to interaction between the mesogens. Like the influence of the solvent polarity, the red shift may be rationalized in terms of the increase in environmental polarity enhancing the relaxation of the excited singlet state to a low-lying intramolecular charge-transfer state or promoting a higher degree of electron transfer in this state [19].

Thermal properties and dynamic mechanical analysis

The glass transition temperature (T_g) of a polymer network is related to the thermal motion of polymer chains, which is affected by the crosslink density and the flexible chains of the network [20, 21]. There are many reports on T_g of LCTs, which confirm that the most important factor influencing T_g is the thermal relaxation of polymer chains rather than phase differences. The T_g's of E*n*E–THPA LCTs are list in Table 3. The value of T_g slightly decreases with the increase of the central spacer length. The increasing length of the central spacer can reduce the crosslink density and increase the flexibility of the chains, both of which can cause the decrease of the T_g.

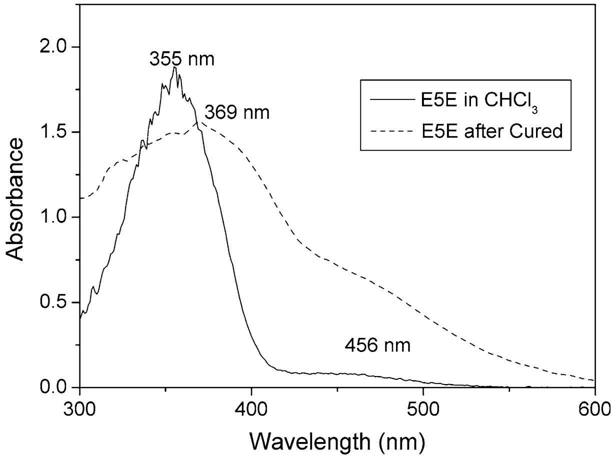

Fig. 6 UV–Vis absorption spectra of monomer E5E in chloroform and E5E LCT

Table 3 Glass transition temperatures (T_g) from DSC and results of thermal degradation of E*n*E–THPA LCTs

Samples	E3E	E4E	E5E	E6E
T_g	90	89	87	82
5% mass loss temperature (°C)	303	303	303	303
Residual weight (%)	27.8	24.6	23.1	22.1

The TGA scans are shown in Fig. 7. The thermal decompositions of all the LCTs begin nearly at the same temperature (220 °C). 5% mass loss temperature of all the scans are all near 303 °C. The length of central spacer imposes no prominent effect on the starting temperature of thermal decomposition, but it impacts the value of the char yield which decreases with the increasing length of the central spacer.

The DTG curve of the E5E LCT shows that the decomposition undergoes three stages. All the other LCTs exhibit the same decomposition behavior. Thermal decomposition generally occurs when the network chains gain sufficient energy to disrupt the backbone covalent bond. The mass loss of azo mesogens usually occurs at a lower temperature due to the easy break of C–N bonds to generate the N_2 gas. For the four LCTs, the inflexions of TGA curves after first stage are all near 340 °C, and the weight loss are about 8.5% which is quite close to the mass fraction of N content . Therefore, the initial stage of the weight loss is due to the escape of N_2. The following two stages are too complicated to analyze only according to the data of thermal gravimetric analysis. Long central spacers decrease the content of the aromatic part, which cause a decrease of residual weight.

The dynamic mechanical properties of the four LCTs are shown in Fig. 8. Like many other thermosets, the storage modulus (E') curves consist of three regions: glass region, glass transition region, and the rubbery region. The storage modulus either at the glass region or at the rubbery region decreases with the increasing length of the central spacer. In the glass state, the LCTs have a high modulus larger than 1 GPa, and the storage modulus quickly decreases in the glass transition region

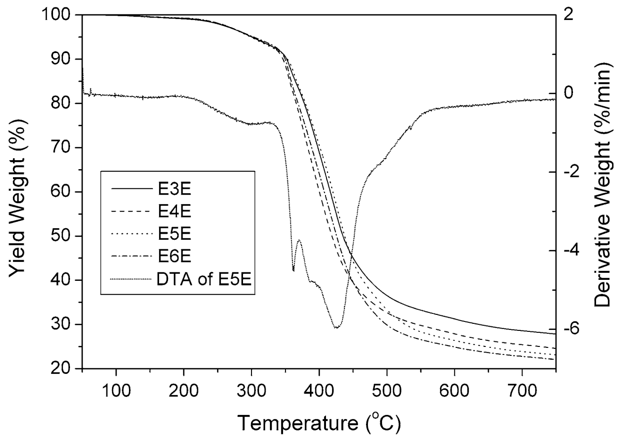

Fig. 7 TGA scanning of cured sample of E3E, E4E, E5E, and E6E

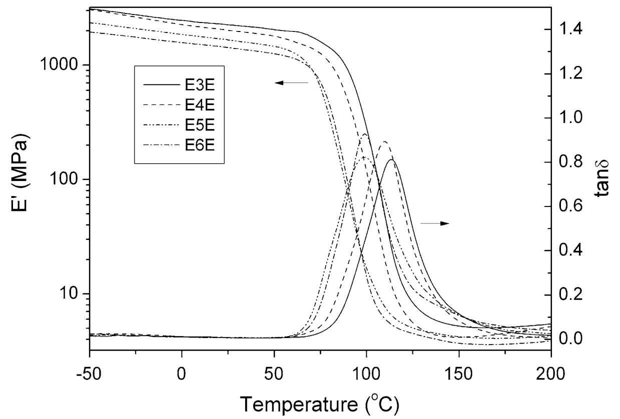

Fig. 8 Storage modulus (E') and loss tangent (tan δ) as determined by DMA for E*n*E LCTs

falling into rubbery region of $E' < 10$ MPa. The tangent of loss angel (tan δ) shows a peak in the transition region corresponding to the α transition (glass transition) and this temperature slightly decreases with the increasing length of central spacer. The increasing length of the central spacer reduces the crosslink density and increases the flexibility of the chains, resulting in the decrease of modulus and transition temperature.

Conclusion

Four dimeric LC epoxy monomers containing azobenzene were synthesized and the mesogenic behavior was studied, which has a good agreement with the reports on dimeric liquid crystals. These monomers were crosslinked in the LC state by THPA.

For large amount of non-mesogenic hardener, only LCTs with nematic phase were obtained. Thermal properties of these LCTs are mainly determined by the chemical structures of the network, and the decomposition of the LCTs undergoes three stages. The UV–Vis absorbance bands of LCTs have a red shift compared to the monomer in $CDCl_3$. The storage modulus either at the glass region or at the rubbery region decreases with the length of the central spacer. The α transition temperature also goes down with the length of the central spacer.

Acknowledgments This project was supported by the National Natural Science Foundation of China (20974121) and the Open Fund from the Key Laboratory of Molecular Engineering of Polymer (Fudan University), Ministry of Education in China.

References

1. Delaire JA, Nakatani K (2000) Linear and nonlinear optical properties of photochromic molecules and materials. Chem Rev 100(5):1817–1845
2. Ikeda T, Mamiya J, Yu YL (2007) Photomechanics of liquid-crystalline elastomers and other polymers. Angew Chem Int Edit 46(4):506–528
3. Ilnytskyi J, Saphiannikova M, Neher D (2006) Photo-induced deformations in azobenzene-containing side-chain polymers: molecular dynamics study. Condens Matter Phys 9(1):87–94
4. Ichimura K (2000) Photoalignment of liquid-crystal systems. Chem Rev 100(5):1847–1873
5. Cui L, Zhao Y, Yavrian A, Galstian T (2003) Synthesis of azobenzene-containing diblock copolymers using atom transfer radical polymerization and the photoalignment behavior. Macromolecules 36(22):8246–8252
6. Tong X, Cui L, Zhao Y (2004) Confinement effects on photoalignment, photochemical phase transition, and thermochromic behavior of liquid crystalline azobenzene-containing diblock copolymers. Macromolecules 37(9):3101–3112
7. Natansohn A, Rochon P (2002) Photoinduced motions in azo-containing polymers. Chem Rev 102(11):4139–4175
8. Finkelmann H, Nishikawa E, Pereira GG, Warner M (2001) A new opto-mechanical effect in solids. Phys Rev Lett 8701(1):015501
9. Harris KD, Cuypers R, Scheibe P, van Oosten CL, Bastiaansen CWM, Lub J, Broer DJ (2005) Large amplitude light-induced motion in high elastic modulus polymer actuators. J Mater Chem 15(47):5043–5048
10. Hogan PM, Tajbakhsh AR, Terentjev EM (2002) UV manipulation of order and macroscopic shape in nematic elastomers. Phys Rev E 65(4):041720
11. Castell P, Galia M, Serra A (2001) Synthesis of new epoxy liquid-crystalline monomers with azo groups in the central mesogenic core. Crosslinking with amines. Macromol Chem Phys 202(9):1649–1657
12. Carfagna C, Amendola E, Giamberini M (1997) Liquid crystalline epoxy based thermosetting polymers. Prog Polym Sci 22(8):1607–1647
13. Shiota A, Ober CK (1997) Rigid rod and liquid crystalline thermosets. Prog Polym Sci 22(5):975–1000
14. Niori T, Adachi S, Watanabe J (1995) Smectic mesophase properties of dimeric compounds. 1. Dimeric compounds based on the mesogenic azobenzene unit. Liq Cryst 19(1):139–148
15. Ribera D, Serra A, Mantecon A (2003) Dimeric liquid-crystalline epoxyimine monomers: Influence of dipolar moments on mesomorphic behavior and the formation of liquid-crystalline thermosets. J Polym Sci A 41(10):1465–1477
16. Shiota A, Ober CK (1996) Synthesis and curing of novel LC twin epoxy monomers for liquid crystal thermosets. J Polym Sci A 34(7):1291–1303
17. Ribera D, Mantecon A, Serra A (2002) Liquid-crystalline thermosets from mesogenic dimeric epoxy resins by tertiary amine catalysis. J Polym Sci A 40(22):3916–3926
18. Ribera D, Serra A, Mantecon A (2003) Liquid-crystal line thermosets by the curing of dimeric liquid-crystal line epoxyimine monomers with 2,4-toluene diisocyanate. J Polym Sci A 41(16):2521–2530

19. King NR, Whale EA, Davis FJ, Gilbert A, Mitchell GR (1997) Effect of media polarity on the photoisomerisation of substituted stilbene, azobenzene and imine chromophores. J Mater Chem 7(4):625–630
20. Pramoda KP, Chung TS, Liu SL, Oikawa H, Yamaguchi A (2000) Characterization and thermal degradation of polyimide and polyamide liquid crystalline polymers. Polym Degrad Stabil 67(2):365–374
21. Zheng YQ, Lu MG, Ren SP, Hang LY, Lan YX (2007) Liquid crystalline Epoxides with long lateral substituents:mechanical and thermal properties. J Polym Sci B 45(20):2835–2841